Incorporation of Nanoparticles Based on *Zingiber Officinale* Essential Oil into Alginate Films for Sustained Release

Nur Ayshah Rosli,[1] German A. Islan,[2] Rosnani Hasham,[3] Guillermo R. Castro[4] and Azila Abdul Aziz[5*]

[1]School of Chemical Engineering, Engineering Campus, Universiti Sains Malaysia, 14300 Nibong Tebal, Pulau Pinang, Malaysia
[2]Centro de Investigación y Desarrollo en Fermentaciones Industriales (CINDEFI), Laboratorio de Nanobiomateriales, Departamento de Química, Facultad de Ciencias Exactas, Universidad Nacional de La Plata (UNLP) – CONICET (CCT La Plata), Calle 47 y 115, (B1900AJI), La Plata, Buenos Aires, Argentina
[3]Department of Bioprocess and Polymer Engineering, School of Chemical and Energy Engineering, Faculty of Engineering, Universiti Teknologi Malaysia, 81310 Johor Bahru, Johor, Malaysia
[4]Nanomedicine Research Unit (Nanomed), Federal University of ABC (UFABC), Santo André, Sau Paulo, Brazil
[5]Department of Chemical and Environmental Engineering, Malaysia-Japan International Institute of Technology, Universiti Teknologi Malaysia, Jalan Sultan Yahya Petra, 54100 Kuala Lumpur, Malaysia

*Corresponding author: r-azila@utm.my

ABSTRACT: *This research focused on the formulation of Ca^{2+} cross-linked alginate (Alg) gels containing Zingiber officinale oil extract (ZOE) loaded into a nanostructured lipid carrier (NLC). The NLC is intended to protect the Zingiber officinale oil against physical and chemical degradation during topical administration to sustain the drug release and reduce drug leakage during storage. The NLC was prepared using hot homogenisation and ultrasonication of glyceryl monostearate. Virgin coconut oil was used as the liquid lipid. The NLC-ZOE had a mean size diameter of 100 nm and a zeta potential value of −40 mV. The ZOE released from NLC followed the Korsmeyer-Peppas model case I (Fickian diffusion). The NLC-ZOE formulation was then incorporated into Alg. The gels were prepared via ionotropic gelation in the presence of calcium. Scanning electron microscopy (SEM) images of Alg films revealed successful*

intercalation of NLC within the Alg matrix. The in vitro ZOE release from NLC-ZOE-Alg occurred in a sustained manner from the cross-linked Alg hydrogels compared to the free NLC. The profiles of NLC-ZOE released from the Alg films depended on the nanoparticles amount. The results demonstrated the importance of designing a local delivery system to entrap and control the release of the bioactive components of ZOE from within the Alg matrix. Ca²⁺ cross-linked Alg gels containing ZOE loaded into NLC was found to be suitable for topical delivery applications, as shown by the sustained release of ZOE from calcium cross-linked Alg films containing NLC that was demonstrated in this study.

1. INTRODUCTION

Over the last decades, herbal extracts are gaining popularity as food supplements because of the many beneficial biological activities. Ginger (*Zingiber officinale*, ZO) is a popular natural flavouring extract with extended use in foods. More than 60 molecules with different physicochemical properties have been identified in ZO extracts (ZOE), but the main components are diarylheptanoids, flavonoids and gingerols. Considering the high number of molecules in the ZO essential oil, it is very difficult to establish the main cellular targets. Besides, ZOE show many beneficial bioactivities such as antioxidant, anti-inflammatory, anti-apoptotic and anticancer, where they were traditionally used in Eastern cultures as a medicinal plant for the treatment of hypertension, arthritis, constipation, etc.[1] However, most of the biologically active molecules of ZOE are highly sensitive to physicochemical degradation when they are exposed to air, light, extreme pH values and heat, which has limited their use in several industrial applications.[2] Since food is the most common route of ginger uptake in the body, the stability of ZOE is limited in the digestive tract of mammalians, since physiological barriers, such as the stomach with very low pH limit the pharmacological effect of ZOE components. In addition, the bioavailability of ZOE is limited based on the "oil" characteristics in an aqueous physiological environment. Also, an increase in the amount of ZOE oral administration, and poor cell targeting of the extract can lead to side effects and low efficiency of the biologically active molecules.

The protection of ZOE from the environment can be accorded using encapsulation technology for extensive use in foods and pharmaceuticals. Essential oil encapsulation to protect the bioactive components can be realised using different strategies.[3] For ginger oils, some of the encapsulation methods include spray drying with whey protein or cashew gum and inulin, electrospinning

of polyethylene oxide, zein and soy proteins, nanoencapsulation of cinnamon-thyme-ginger composite essential oil via ionic gelation of chitosan with polyphosphate and preparation of chitosan microcapsules containing red ginger oleoresin using the emulsion crosslinking method.[4–8] However, these reported techniques and/or materials are relatively complex, time-consuming and expensive for medium to large scale use.

Since ZO is water insoluble, the use of lipids can be a simple and cheap strategy for encapsulation. The use of high-speed homogenisation to prepare liposomes with sunflower and lecithin containing ZOE has been reported.[9] The synthesis of solid lipid nanoparticles composed of medium chain triglyceride and glyceryl monostearate for the encapsulation of one of the components of ZO, [6]-shogaol or [1-(4-hydroxy-methoxyphenyl)-4-decenone] through the high-pressure homogenisation technique has also been recently reported.[10]

Solid lipid nanoparticles (SLN) pave the way for a new strategy for molecular delivery since they possess a solid structure under physiological conditions and overcome the structural instability of liposomes at different environmental conditions, which is related to an unpredictable release kinetic. However, the main disadvantage of SLN is the crystal structure of the particle that sometimes leads to partial or total extrusion of the cargo molecule.[11] Nanostructured lipid carriers (NLC) is a new generation of lipid transporters for molecular delivery. NLCs are solid lipid structures containing a mixture of solid and liquid lipids that can encapsulate molecules with diverse physicochemical properties. NLCs are suitable candidates to act as carriers for hydrophobic compounds and have been previously applied in various drug delivery fields, particularly those with complex natural extracts such as ZOE.[12]

A strategy to avoid problems associated with oral administration of molecules is transdermal or topical drug delivery. Patches for molecular delivery offer many advantages because they are easy to handle, wearable, non-invasive and painless, where no trained personnel or adequate infrastructure is required. The molecules administered using patches are mainly applied on wounds, burns or normal skins and can be released by triggering the local and/or systemic biological activities.[13]

Among biodegradable polymers, alginate (Alg) is one of the most popular choices for molecular encapsulation because of its excellent properties. Alg is a linear anionic polysaccharide, consisting of β-1,4-D-mannuronic acid (M-block) and α-1,4-L-glucuronic acid (G-block), which can be obtained from brown seaweeds such as *Laminaria digitata* and *L. hyperboria*.[14] Alg can form gel structures when the sodium ion is replaced by multivalent cations such as

Ca^{2+}, Zn^{2+}, etc., due to the formation of cationic bridges between the guluronic-rich entities along the biopolymer backbone, which is commonly called egg-box structure. Alg has been used to produce an effective controlled release carrier such as matrices, beads and microcapsules since it is considered as GRAS (Generally Regarded as Safe by FDA, USA). Alg allows the entrapment of a wide range of environmentally sensitive molecules since its interior is known to be chemically inert. Alg gels offer the following advantages: a synthesis process that is free of organic solvents and under mild experimental conditions, high gel porosity, which allows high diffusion rates of macromolecules, dissolution and biodegradation of the system under normal physiological conditions. Alg films allow highly localised delivery of small amounts of active ingredients and hence, desirable proper local concentrations over sustained time periods with minimal tissue exposure at other sites can be achieved.

The aim of the present study was to develop a patch based on a novel hybrid platform for the delivery of ZOE encapsulated in NLC and entrapped into Alg films. The physicochemical characteristics of the films were carefully characterised to study the possibility of using the films for topical delivery. The properties of NLC-ZOE were analysed through transmission electron microscopy, dynamic light scattering and thermogravimetry. The kinetic release of ZOE from NLC was analysed using structured models. Surface and cross sections of Alg films containing NLC-ZOE were analysed through scanning electron microscopy and the ImageJ program. The kinetic release of NLC-ZO from Alg films was also studied.

2. EXPERIMENTAL

2.1 Materials

Tween 80, Sephadex G-50 and soy lecithin were obtained from Sigma-Aldrich (Selangor, Malaysia). The liquid lipid, namely virgin coconut oil, was obtained from the Institute of Bioproduct Development (Universiti Teknologi Malaysia, Malaysia). ZO oil was purchased from Wellness Original Ingredient (Selangor, Malaysia). Other chemicals and solvents used such as methanol and glyceryl monostearate were of analytical reagent grade and pharmaceutical grade, where they were obtained from Sigma-Aldrich (Buenos Aires, Argentina).

2.2 Encapsulation of ZO Oil in a NLC

The NLC encapsulating ZO oil extract (NLC-ZOE) were prepared using a hot homogenisation and ultrasonication method. The lipid phase was formed using glyceryl monostearate and virgin coconut oil, while the aqueous phase consisted of water, Tween 80 and soy lecithin. The mixing of the aqueous and lipid phases formed the pre-emulsion with the assistance of heat. Upon homogenisation, ZO oil was added and followed by ultrasonication of the pre-emulsion.

The theoretical loading (DL, %) was calculated as follows:

$$DL\ (\%) = \frac{\text{Mass of extract incorporated (mg)}}{\text{Lipid mass (mg)}} \times 100$$

2.3 Alg Film Deposition and Cross-Linking

Sodium alginate (2.0%) was dissolved in 50 ml aliquots of ultrapure water and mixed with NLC-ZO at a ratio of 1:9. The gel cross-linking was performed in 1.0 M calcium chloride solution containing propylene glycol for 30 min. The solution was then removed, and the Alg films were rinsed for 10 sec in ultrapure water and dried using a freeze drier.

2.4 Dynamic Light Scattering (DLS)

Particle size, zeta potential and polydispersity index analyses were performed via DLS using Malvern Zetasizer Nano S equipment (Malvern Instruments, Worcestershire, UK). All samples were diluted using distilled water and vortexed for 30 sec to generate a suitable scattering intensity. NLC measurements were performed in triplicate at 25°C. The refractive indexes of particles and water were 1.54 and 1.33, respectively, where they were used to calculate particle size distributions and the polydispersity index (PI).

2.5 Transmission Electron Microscopy (TEM)

TEM analysis was performed using a Jeol-1200 EX II-TEM microscope (Jeol, Columbia, MD, USA). At a ratio of 1:100, nanoparticle dispersions were diluted with ultrapure Milli-Q® water, and 10 µl of the formulation was spread onto a Copper grid of 400 mesh. After incubation, a paper filter was used to remove sample excess. One drop of phosphotungstic acid was added to the grid for contrast enhancement and the grid was incubated at 25°C for one min before excess removal. Finally, the grid was dried at room temperature.

2.6   Scanning Electron Microscopy (SEM)

Biopolymeric films containing NLC were freeze-dried. The films were non-conductive electron samples and were prepared by sputtering the surface with gold using a Balzers SCD 030 metalliser. The gold layer thickness was between 150 A and 200 A. The surface and morphology were determined using a scanning electron microscope (Philips SEM 505) and processed by an image digitiser program [Soft Imaging System ADDA II (SIS)]. ImageJ version 3.8 was used for post-processing and analysing the image after image acquisition.[16] ImageJ detected the significant size differences between particles from the SEM microphotographs. Additionally, the morphology of particle size distribution and particle size can be analysed. The surface roughness was estimated from simulated intensity and height curves, while neglecting the actual roughness effects.

2.7   Fourier Transform Infrared (FTIR) Spectroscopy

FTIR spectra were obtained using a Nicolet 6700 (Thermo Scientific, Inc., Waltham, Ma, USA) spectrometer. The attenuated total reflectance (ATR) mode was used to record spectra over the range of 450 cm^{-1}–4000 cm^{-1} at 2 cm^{-1} resolution.

2.8   In Vitro Release Study

Dried samples of NLC-ZOE or NLC-ZOE-Alg films were placed in a 1.5 ml plastic vial containing 20 mM phosphate buffered saline (PBS, pH 6.5), which was then placed in a shaker at 100 rpm at room temperature. At predetermined time intervals, 100 μl samples were withdrawn and replaced with fresh medium to maintain the original volume. The amount of NLC released from the Alg film was determined using a UV-Vis spectrophotometer at 500 nm. The process was validated using a PBS solution containing only a thin Alg film as a control. The kinetic modelling parameter was determined using non-linear curve fitting method using SOLVER tool in Microsoft Excel 2016.

3.   RESULTS AND DISCUSSION

NLC-ZO was successfully prepared using the hot homogenisation and ultrasonication method. Size, polydispersity index and zeta potential of the nanoparticles were analysed using DLS. The NLC-ZOE formulation showed the particles' size was in the range of 90 nm to 100 nm with a polydispersity

index of 0.150 in ultrapure water and zeta potential of −40 mV. TEM images of NLC-ZOE showed spherical nanoparticles with a narrow particle size distribution (as shown in Figure 1).
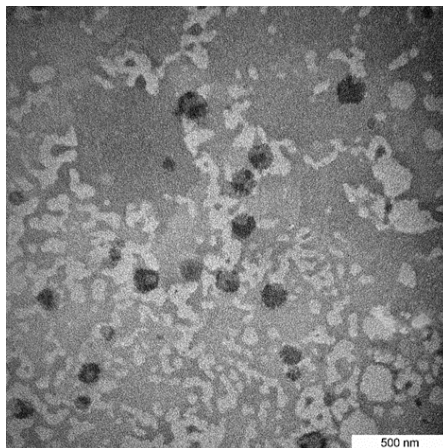

Figure 1:   Transmission electron microscopy microphotography of nanostructured lipid carrier containing ZO essential oil extract (magnification of 50 000x).

Stability studies of NLC-ZOE performed for 3 months showed small changes in particle size with averages of 96.5 nm and 92.3 nm at 25°C and 10°C, respectively (as shown in Figure 2[A]). Also, the average PI of NLC-ZOE was 0.18 and 0.17 at 25°C and 10°C respectively (as shown in Figure 2[B]). These results indicate a high stability in NLC-ZOE formulation. The good stability achieved for NLC-ZOE was due to the blend of surfactants used for the preparation of NLC, which were Tween 80 and soy lecithin. The stearic repulsion is the major colloidal interaction among NLC particles when stabilised with non-ionic surfactants only.[16] Tween 80 is a water-soluble and non-ionic synthetic surfactant with HLC value of 15, while lecithin is made up of hydrophobic molecules with HLC value of 8 and not suitable for stabilising NLC individually. Therefore, the combination of both Tween 80 and soy lecithin have significantly lowered the interfacial tension and decreased the coalescence of dispersing droplets in the system by calculating the ratio of hydrophobic to hydrophilic portion of the molecule.[17]

It is also noted that an increment in particle size and polydispersity index (PDI) were recorded on the 30th day; however, the increment was statistically insignificant ($P > 0.005$). The PDI increased but was still in good homogeneity region. The PDI of less than 0.5 shows that the samples were monodisperse and

homogenous. The slight increment was probably due to the agglomeration and aggregation that occurred on the NLC-ZOE suspension over time, particularly for the sample that was stored in room temperature. On the other hand, the heterogeneous distribution of the nanoparticles could also cause an increase of agglomerates.[18]
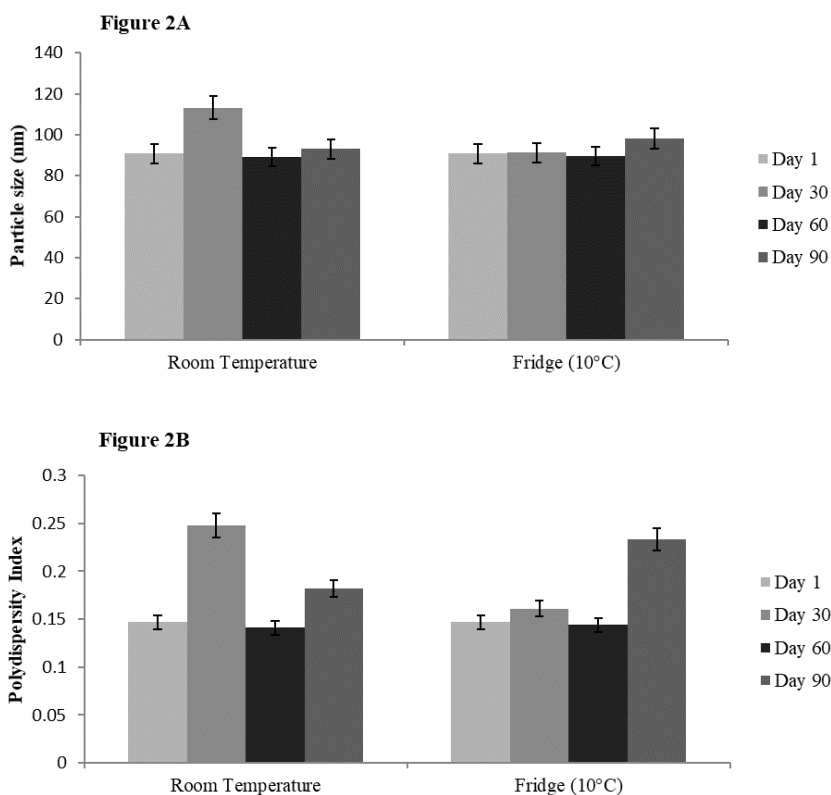

Figure 2: Particle size (A) and polydispersity index (B) of NLC-ZOE stored at 25°C and 10°C for 90 days. Data is presented in the form of mean ± standard deviation (SD) ($n = 3$).

The thermogravimetric analysis of NLC showed a minimum peak located at 73°C–75°C, which may be correlated with the melting point of glyceryl monostearate. Meanwhile, for the NLC containing ZO oil extract, the melting point decreased by about 5ºC with a minimum of 66ºC–68ºC (as shown in Figure 3). The decrease of the melting point can be explained by the interference of the crystalline structure of glyceryl monostearate by the presence of ZOE liquid. Muller et al. reported that the lipid blend of NLC showed a melting point depression compared to the original solid lipid, but the obtained blend

was also solid at body temperature.[19] On the other hand, the study by Zheng et al. revealed different slope steepness as the liquid lipid ratio increased in the NLC formulation.[20] With the increase of liquid lipid (9:1 to 8:2), the peak gradually broadened and decreased in intensity, which indicates reduced crystallinity. Hence, it can be concluded that the liquid lipid molecularly dispersed in the solid lipid matrix.
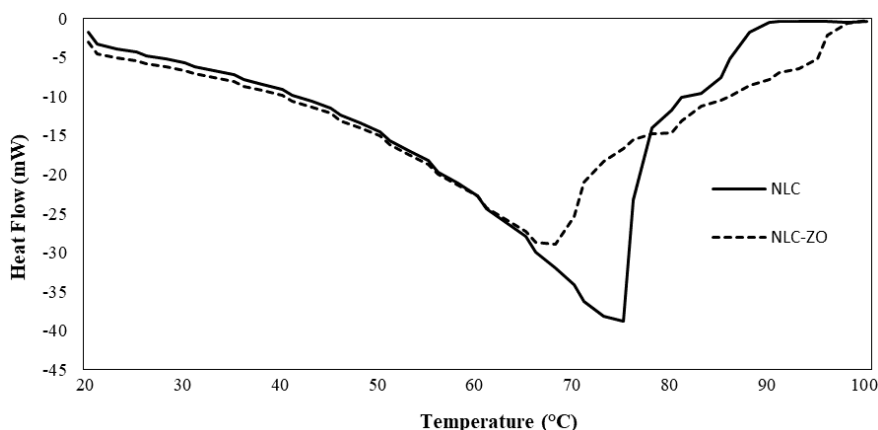

Figure 3:   Thermogravimetric analysis of nanostructured lipid carriers without (——) and with (----) Zingiber officinale oil extract, respectively.

ZOE is a complex mixture of more than 50 different molecules and consequently it is difficult to properly assign specific spectroscopy bands.[21] However, characteristic bands of ZOE oil can be spectroscopically assigned. FTIR spectroscopy of ZOE showed strong bands at 2961.28 cm^{-1} and 2923.04 cm^{-1} that could be assigned to HO stretching and H-bonding of carboxylic acids; and that at 2870.77 cm^{-1} to the $\upsilon_{C-H,}$ the 1728.91 cm^{-1} band could be assigned to the $\upsilon_{C=O}$ and the ones at 1641.18 cm^{-1} to the alkene vinyl group; the bands at 1514.19 cm^{-1} and 1448.24 cm^{-1} can be attributed to $\upsilon_{C=C}$ related to the aromatic rings of ZOE. The 1377.23 cm^{-1} band can be assigned to $\delta_{-CH3sym}$ of alkane methyl groups and that at 1215.86 cm^{-1} to υ_{C-O-C} of vinyl ether. The bands at 985.93 cm^{-1}, 878.35 cm^{-1}, 816.73 cm^{-1}, 795.46 cm^{-1} and 728.84 cm^{-1} denoted the appearance of aliphatic amines, carboxylic acid, alkenes, alkyl halides and aromatic groups that were present in ZOE (as shown in Figure 4). Meanwhile, the FTIR spectrum of the ZOE completely disappeared when it was formulated in NLC. The FTIR spectra of NLC and NLC-ZOE displayed similar peaks. Particularly, the FTIR spectrum of glyceryl monostearate showed that the stretching bands (υ_{max}) at 3312.25 cm^{-1} and 3314.33 cm^{-1} could be assigned to the OH group, while the bands at 2926.3 cm^{-1} and

2926.51 cm^{-1} attributed to CH asymmetric stretching at 2856 cm^{-1} to CH symmetric stretching at 1637 cm^{-1} to $\nu_{C=O}$, and at 108.69 cm^{-1} and 1087.82 cm^{-1} to the C-O stretching for NLC and NLC-ZOE, respectively. Additionally, the weak bending bands of glyceryl monostearate appeared at 1462.71 cm^{-1} and 1457.29 cm^{-1} for asymmetric δ, while the bands at 1377.41 cm^{-1} and 1372.40 cm^{-1} were for symmetric δ of NLC and NLC-ZO, respectively (as shown in Figure 4).[21,22]

Figure 4: FTIR spectroscopy of ZOE (red), nanostructured lipid carrier (blue) and NLC-ZOE formulation (black).

Studies of ZOE kinetic release from NLC at 25ºC showed a hyperbolic release profile up to 50 h. The ZOE release from the nanoparticles was about 39% and 63% at 1 h and 8 h, respectively (as shown in Figure 5). The kinetic release of ZOE from NLC was analysed using equations from different controlled release kinetic models (as shown in Table 1). The model with the better fit was the Korsmeyer-Peppas model with a 0.93 correlation coefficient, followed by 0.91 for the Higuchi model. Both models have equation similarities, but the Korsmeyer-Peppas model predicts the mechanism of molecular release that is represented by *n* coefficient in the equation. Values of $n \leq 0.45$ indicate a classical Fickian diffusion-controlled molecular release or Case I type, which is the ZO release from NLC with R^2 of 0.216.[23]

Table 1: Evaluation of ZO essential oil released from NLC using structured models

Model	Formula	NLC-ZO release equation	
		Equation	R^2 adjusted
Zero order	$M_t/M_\infty = k\,t$	$M_t/M_\infty = 0.00471\,t$	0.85
First order	$M_t/M_\infty = 1 - e^{kt}$	$M_t/M_\infty = 1 - e^{0.001t}$	0.76
Higuchi	$M_t/M_\infty = k\,t^{1/2}$	$M_t/M_\infty = 0.045t^{1/2}$	0.91
Hixson-Crowell	$M_t/M_\infty = k_1 t + k_2 t^2 + k_3 t^3$	$M_t/M_\infty = (9.2 \times 10^{-6})\,t +$ $0.0033\,t^2 + 0.01\,t^3$	0.59
Weibull	$M_t/M_\infty = 1 - e^{-(t-\alpha)m/\beta}$	$M_t/M_\infty = 1 - e^{-(t-0.1)}$	0.44
Korsmeyer-Peppas	$M_t/M_\infty = k\,t^n$	$M_t/M_\infty = 0.149\,t^{0.216}$	0.93

The inclusion of different amounts of NLC-ZOE into Alg films can be observed in SEM micrographs (as shown in Figure 6). They showed a smooth surface on Alg films without NLC, meanwhile rough film surfaces increased with the addition of NLC-ZOE to Alg film samples. The appearance of sphere-like nanoparticles with slight aggregation on Alg surfaces was observed (as shown in Figure 6). The aggregation of NLC-ZOE could be due to the freeze-drying process.
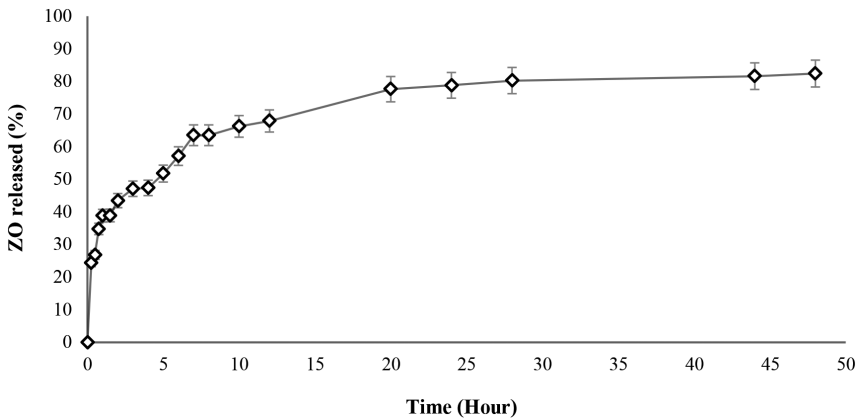

Figure 5: Kinetic release of ZOE from NLC at 25°C. The values represent the mean ± SEM ($n = 3$).

SEM micrographics of the film cross section for Alg films without and with different concentrations of NLC are shown in Figure 7. The increased concentration of NLC in the films is evidenced by the emergence of globular structures inside the films. The number of globular structures may be correlated with the increase in NLC amounts loaded into the films from ratio of 1/10 to 1/1.

Statistical surface analysis of SEM micrographs of the Alg films through ImageJ showed the roughness doubled (from 13 to 26) due to the low number of nanoparticles (i.e., 1/10, w/w) loaded into the Alg film (as shown in Figures 8 and 9). A further increase of NLC amounts (i.e., 1/3, 1/1, w/w) loaded into the Alg films increased the surface roughness by only 10%–13% because the nanoparticles diffused into the films, as displayed in the SEM images of the scaffold cross section (as shown in Figure 7).

SEM micrographics of the film cross section for Alg films without and with different concentrations of NLC are shown in Figure 7. The increased concentration of NLC in the films is evidenced by the emergence of globular structures inside the films. The number of globular structures may be correlated with the increase in NLC amounts loaded into the films from ratio of 1/10 to 1/1.
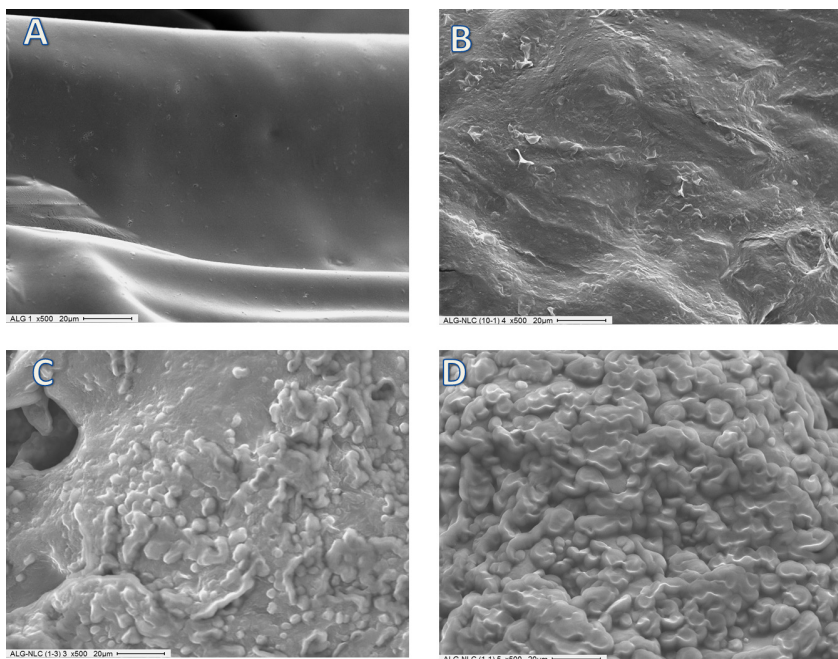

Figure 6: Scanning electron microscopy microphotographs of 2.0% alginate films (500×) without and with different mass of nanostructure lipid carriers containing ZO extract: (a) and (b) 1/10; (c) 1/3 and (d) 1/1, respectively.

The kinetic release of NLC-ZOE from Alg films for about 12 days showed different profiles according to the amount of NLC loaded into the film (as shown in Figure 10). The release of the nanoparticles was linear ($R^2 = 0.93$) when low amounts of NLC were loaded into the Alg gels, which may be correlated with the respective SEM images in which most of the particles were on the surface of the Alg film (as shown in Figures 6[B] and 7[B]). At an intermediate amount of NLC-ZOE loaded into the film, the release kinetics was exponential in the first part of the curve up to 7–8 days and later the release decreased drastically, which can be associated with the high number of nanoparticles located at the surface of the films and the low amount inside them (as shown in Figures 6[C] and 7[C]). Meanwhile, the NLC release from the Alg films became hyperbolic when a high number of nanoparticles were loaded into the film (i.e., 1/1) because the nanoparticles were not only on the film surface but also inside the film, as displayed in the SEM micrographs (as shown in Figures 6[D] and 7[D]).
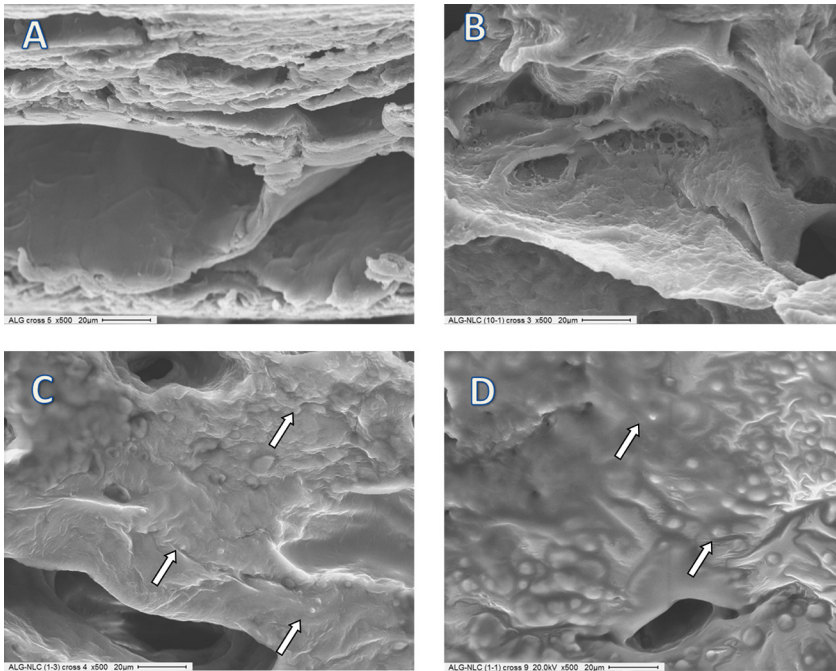

Figure 7:   Scanning electron microscopy microphotographs of 2.0% alginate cross section films (500x) without and with different mass of nanostructured lipid carriers containing ZO extract: (a) and (b) 1/10; (c) 1/3 and (d) 1/1, respectively.

Alg gels have been studied regarding the delivery of a variety of therapeutic agents.[24] They are most useful if the kinetics of the drug release can be tuned by manipulating the primary or secondary bond between the therapeutic agents and the Alg.[25] In this work, a novel hybrid platform for entrapping ZOE encapsulated in NLC into Alg films was investigated. The findings from this study revealed that sustained release from the resulting hybrid Alg matrix is possible. The profiles of NLC-ZOE released from the Alg films depended on the position of the nanoparticles within the Alg films, which were correlated with the amount of NLC-ZOE entrapped in the Alg matrix. The results demonstrated the possibility of designing a local delivery system to control the release of bioactive components of ZOE from within the Alg matrix. Due to the possibility of tuning the hybrid system to obtain the desired profile of sustained release, Ca^{2+} cross-linked Alg gels containing ZOE loaded into NLC was found to be suitable for topical delivery applications.
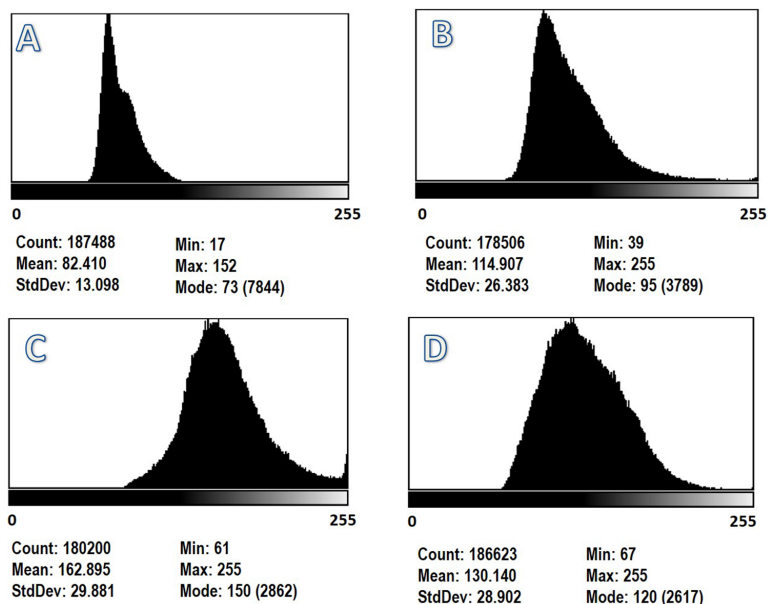

Figure 8:   Profiles of alginate films obtained from SEM microphotographs with ImageJ program without and containing different amounts of nanostructured lipid carriers: (a) no NLC; (b) 1/10 NLC; (c) 1/3 NLC and (d) 1/1 NLC.
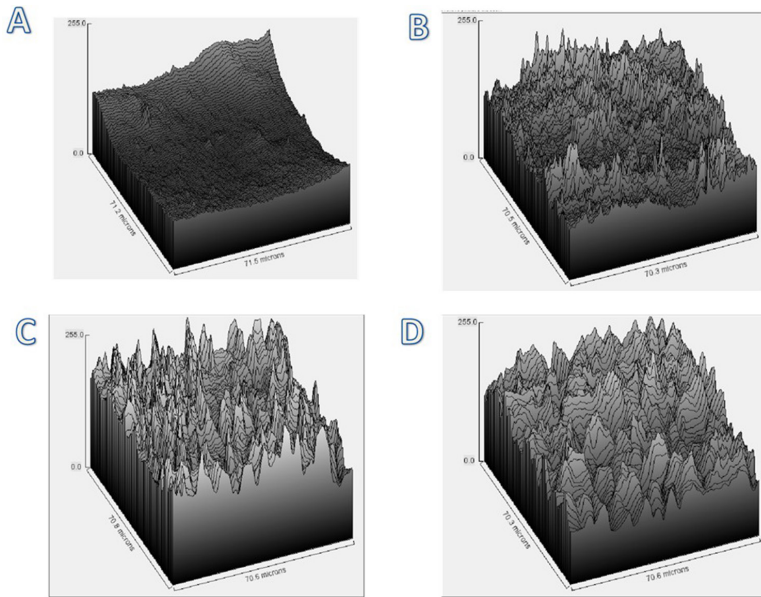
Figure 9:   3D Alg film images obtained of SEM microphotographs with ImageJ program without and containing different amounts of nanostructured lipid carriers: (a) no NLC; (b) 1/10 NLC; (c) 1/3 NLC and (d) 1/1 NLC.
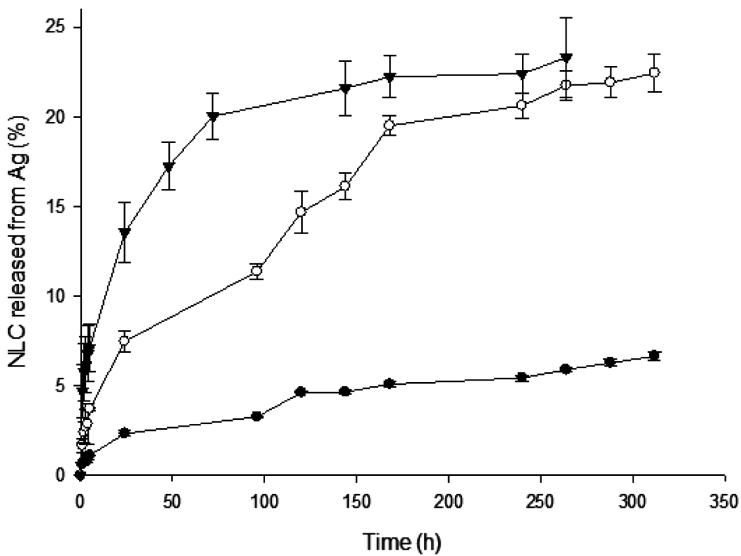

Figure 10: Kinetic release of NLC-ZOE from alginate films containing different amounts of nanoparticles (w/w).
Note: (▼) NLC 1/1; (○) NLC 1/3 and (●) NLC 1/10.

4.   CONCLUSIONS

The NLC platform was able to encapsulate and release ZOE with specific kinetics and high stability. The small nanoparticle diameter and polydispersity guarantee the proper delivery of the cargo through Fickian diffusion, as predicted by the Korsmeyer-Peppas structured model. The NLC-ZOE was stable in a wide range of temperatures for at least 90 days. SEM micrographs revealed the presence of NLC-ZOE on the surface and when the amount of NLC-ZOE increased, it was also present inside the Alg matrix. Also, the profiles of NLC-ZOE release from the Alg films depended on the nanoparticle amount. The results demonstrated the importance of designing a local delivery system to entrap and control the release of the bioactive components of ZOE within the Alg matrix.

5.   ACKNOWLEDGEMENTS

6.   REFERENCES

1.   Srinivasan, K. (2017). Ginger rhizomes (*Zingiber officinale*): A spice with multiple health beneficial potentials. *PharmaNutrition*, 5(1), 18–28. https://doi. org/10.1016/j.phanu.2017.01.001

2.   Bhattarai, S. et al. (2001). The stability of gingerol and shogaol in aqueous solutions. *J. Pharm. Sci.*, 90(10), 1658–1664. https://doi.org/10.1002/jps.1116

3.   Rodríguez, J. et al. (2016). Current encapsulation strategies for bioactive oils: From alimentary to pharmaceutical perspectives. *Food Res. Int.*, 83, 41–59. https://doi.org/10.1016/j.foodres.2016.01.032

4.   Fernandes, R. V. D. B. et al. (2017). Microencapsulated ginger oil properties: Influence of operating parameters. *Dry. Technol.*, 35(9), 1098–1107. https://doi .org/10.1080/07373937.2016.1231690

5.   De Barros Fernandes, R. V. et al. (2016). Cashew gum and inulin: New alternative for ginger essential oil microencapsulation. *Carbohydr. Polym.,* 153, 133–142. https://doi.org/10.1016/j.carbpol.2016.07.096

6.   Da Silva, F. T. et al. (2018). Action of ginger essential oil (*Zingiber officinale*) encapsulated in proteins ultrafine fibers on the antimicrobial control *in situ*. *Int. J. Biol. Macromol.*, 118(A), 107–115. https://doi.org/10.1016/j.ijbiomac.2018.06 .079

7.   Hu, J. et al. (2018). Preparation and properties of cinnamon-thyme-ginger composite essential oil nanocapsules. *Ind. Crops Prod.*, 122, 85–92. https://doi. org/10.1016/j.indcrop.2018.05.058

8.   Jayanudin et al. (2019). Preparation of chitosan microcapsules containing red ginger oleoresin using emulsion crosslinking method. *J. Appl. Biomater. Funct. Mater.*, 17(1), 1–9. https://doi.org/10.1177/2280800018809917

9.   Ganji S., & Sayyed-Alangi S. Z. (2017). Encapsulation of ginger ethanolic extract in nanoliposome and evaluation of its antioxidant activity on sunflower oil. *Chem. Pap.*, 71, 1781–1789. https://doi.org/10.1007/s11696-017-0164-1

10.   Wang, Q. et al. (2018). Enhanced oral bioavailability and anti-gout activity of [6]-shogaol-loaded solid lipid nanoparticles. *Int. J. Pharm.*, 550(1–2), 24–34. https://doi.org/10.1016/j.ijpharm.2018.08.028

11.   Islan, G. A. et al. (2017). Development and tailoring of hybrid lipid nanocarriers. *Curr. Pharm. Des.*, 23(43), 6643–6658. https://doi.org/10.2174/138 16128236661711151110639

12.   Rosli, N. A. et al. (2018). Design and physicochemical evaluation of nanostructured lipid carrier encapsulated zingiber zerumbet oil by D-optimal mixture design. *J. Teknol.*, 80(3), 105–113. https://doi.org/10.11113/jt.v80.11268

13.   Santos, L. F. et al. (2018). Biomaterials for drug delivery patches. *Eur. J. Pharm. Sci.*, 118, 49–66. https://doi.org/10.1016/j.ejps.2018.03.020

14.   Sehgal, R. et al. (2019). Alginates: General introduction and properties. In Ahmed S. (ed). *Alginates: Applications in the biomedical and food industries*. New Jersey: John Wiley and Sons, 3–20.

15.   Rasband, W. (2007). ImageJ 1.34 s. Image processing and analysis in Java. National Institutes of Health, Bethesda, Maryland. Retrieved 25 June 2020, https://ui.adsabs.harvard.edu/abs/2012ascl.soft06013R/abstract

16.   Tamjidi, F. et al. (2013). Nanostructured lipid carriers (NLC): A potential delivery system for bioactive food molecules. *Innov. Food Sci. Emerg. Technol.*, 19, 29–43. https://doi.org/10.1016/j.ifset.2013.03.002

17.   Griffin, W. C. (1954). Calculation of HLB values of non-ionic surfactants. *J. Soc. Cosmet. Chem.*, 5, 249–256.

18.   Moreno-Sastre, M. et al. (2016). Stability study of sodium colistimethate-loaded lipid nanoparticles. *J. Microencapsul.*, 33(7), 636–645. https://doi.org/ 10.1080/02652048.2016.1242665

19.   Müller, R. H. et al. (2002). Solid lipid nanoparticles (SLN) and nanostructured lipid carriers (NLC) in cosmetic and dermatological preparations. *Adv. Drug Deliv. Rev.*, 54(S1), S131–S155. https://doi.org/10.1016/S0169-409X(02)00118-7

20.   Zheng, M. et al. (2013). Formulation and characterization of nanostructured lipid carriers containing a mixed lipids core. *Colloids Surf. A Physicochem. Eng. Asp.*, 430, 76–84. https://doi.org/10.1016/j.colsurfa.2013.03.070

21.   Purnomo, H. et al. (2010). The effects of type and time of thermal processing on ginger (Zingiber officinale Roscoe) rhizome antioxidant compounds and its quality. *Int. Food Res. J.*, 17(2), 335–347.

22.   Devi, A. et al. (2017). Ginger extract as a nature based robust additive and its influence on the oxidation stability of biodiesel synthesized from non-edible oil. *Fuel*, 187: 306–314. https://doi.org/10.1016/j.fuel.2016.09.063

23.   Korsmeyer R. W. et al. (1983). Mechanisms of solute release from porous hydrophilic polymers. *Int. J. Pharm.*, 15, 25–35.

24.   Croisfelt, F. M. et al. (2019). Modified-release topical hydrogels: A ten-year review. *J. Mater. Sci.*, 54, 10963–10983. https://doi.org/10.1007/s10853-019-03557-x

25.   Lee K. Y. & Mooney D. J. (2012). Alginate: Properties and biomedical applications. *Prog. Polym. Sci.*, 37(1), 106–126. https://doi.org/10.1016/j.progpolymsci.2011.06.003